American Mineralogist, Volume 84, pages 70–77, 1999

Trace element analysis with the electron microprobe: New data and perspectives

MICHEL FIALIN,[1,*] HUBERT RÉMY,[1] CLAUDINE RICHARD,[1] AND CHRISTIANE WAGNER[2]

[1]Centre de Microanalyse Camparis, Université Pierre et Marie Curie, 4 Place Jussieu, 75252 Paris cedex 05, France
[2]Laboratoire de Pétrologie, ESA 7058-CNRS, Université Pierre et Marie Curie, 4 Place Jussieu, 75252 Paris cedex 05, France

ABSTRACT

This work presents a procedure developed for trace element analysis using the electron microprobe (EMP). The method is demonstrated by analysis of seven glasses prepared from reference rock powders, with compositions of granite, granodiorite, andesite, diabase, and basalt. The melting process was adapted to prevent the loss of volatile elements and to obtain homogeneous samples. A routine procedure for analysis of major and minor (above 1000 ppm) elements yielded results in fairly good agreement with published values. The methods presented in this study produced detection limits as low as: (1) 6–8 ppm when the $K\alpha$ peaks of transition metals of the first row (Cr and Ni) were used; (2) 23 ppm with soft $L\alpha$ peaks (Y, Zr, and Sr); (3) 15 ppm with high-energy $L\alpha$ peaks (rare earth elements); and (4) 35 ppm with the $M\alpha$ peaks of heavy elements (Pb and Th). These limits were achieved after total counting times (peak + two background measurements) of about 15 min with a beam of 35 kV and 500 nA. Precision ($\pm 2\sigma$) on the weight percent concentrations was below 50% for concentrations above 13 ppm for group 1 elements, 35 ppm for group 2, 25 ppm for group 3, and 55 ppm for group 4. In the present work, a commercial software package was adapted for quantitative trace element analysis. One modification addresses beam-sensitive materials for which the long counting times required for measurements need to be divided into subsets (10–20 s count), each acquired from different sites of the sample surface, to minimize damage. This analytical mode is referred to as ''multi-site'' mode.

INTRODUCTION

In recent years numerous studies have shown that information related to the source and evolution of rock systems may be recorded at a microscale in minerals. However, the bulk analytical techniques that allow the detection of elements at very low concentrations give only average mineral compositions. Measurements at the scale of individual phases are commonly required to characterize complex geochemical processes. For this purpose, in situ microanalytical techniques have become essential tools for major, trace element, and isotopic determinations. For example, ion microprobe (SIMS) techniques permit the study of element migration at the mineral scale (Vannucci et al. 1994) or the interaction of different metasomatic agents with mantle materials (Johnson et al. 1996). Similarly, Lloyd et al. (1996) determined the distribution of LREE in apatite, perovskite, and titanite with the electron microprobe (EMP). They estimated the detection limits to be on the order of 0.1–1 wt%, with a precision of ±20% for concentration at the lowest levels.

The aim of the present study was to show that EMP analysis, which is a routine analytical technique for major and minor elements, also can be used for trace element analysis provided an improved analytical procedure is utilized. No systematic use of expensive and low-accessibility microbeam instruments or related techniques designed for trace element analysis [e.g., ion microprobes for secondary ion mass spectrometry (SIMS); van de Graaff accelerators for proton induced X-ray emission (PIXE); synchrotron facilities for synchrotron radiation induced X-ray emission (SXRF)] is required when the EMP, a basic instrument widespread in mineralogy and petrology, is available. Although trace element analyses is shown to be possible in this paper, the critical question is how the information is to be used. Because errors necessarily increase at low concentrations, using EMP determinations to define, for instance, a distribution coefficient of LREE at the 20 ppm level between glass and crystal, would give a result with very large errors and thereby be almost useless. On the other hand, simply showing the presence of LREE at the 20 ppm level might be easily shown with the EMP.

This paper is part of a larger study on the accuracy and precision that can be achieved with the EMP for trace elements in minerals and glasses. Analyses of some trace elements (Cr, Ni, Y, Zr, Sr, La, Nd, Ce, Sm, Pb, and Th) in reference glasses from a large range of compositions are given here.

BASIC CONCEPTS

The concept of detection level (see terminology and references on counting statistics applied to the EMP in

* E-mail: fialin@ccr.jussieu.fr

0003–004X/99/0102–0070$05.00

Merlet and Bodinier 1990) is a useful way to evaluate the performance of an analytical method. By definition, a characteristic line emitted from an element with low concentration is not detected unless the signal level, n_C, reaches three standard deviations of the distribution $n_P - n_B$, where n_P and n_B are the accumulated counts on the peak (PK) and background (BG), respectively. Hence, n_c can be expressed as:

$$n_C = 3\cdot\sigma_{P-B} = 3\cdot(\sigma_P^2 + \sigma_B^2)^{1/2}. \quad (1)$$

When the BG has been determined accurately by averaging many measurements (N = total number of measurements) collected from a blank, $\sigma_B \ll \sigma_P$ [$\sigma_B = [\Sigma\ (n_{Bi} - \langle n\rangle)^2/N]^{1/2}$, where $\langle n\rangle$ is the average value of the distribution $n_{B1}, \ldots, n_{Bi}, \ldots, n_{BN}$; $\sigma_P = n_P^{1/2} \cong n_B^{1/2}$, owing to the near equality of both poissonian distributions n_P and n_B]. Thus, n_C can be written:

$$n_C = n_P - n_B = 3\cdot n_B^{1/2}. \quad (2)$$

Equation 2 gives the lowest PK that can be extracted from the BG, n_B. In most cases, both PK and BG intensities are measured on the unknown with identical counting times ($\sigma_P \cong \sigma_B$), which leads to the well-known formula (Goldstein et al. 1986; Reed 1995):

$$n_P = n_B + 3\cdot(2\cdot n_B)^{1/2} \quad (3)$$

where $n_P = I_P\cdot t_{min}$ and $n_B = I_B\cdot t_{min}$. I_P and I_B are, respectively, the PK and BG count rate in counts per second (c/s).

The minimum counting time required to confirm peak detection, t_{min}, is thus given by:

$$t_{min} = 18\cdot I_B/(I_P - I_B)^2. \quad (4)$$

Ancey et al. (1979) gave an approximate formula for t_{min}:

$$t_{min} = \lambda(\alpha,\beta)\cdot(I_P + I_B)/(I_P - I_B)^2 \quad (5)$$

where $\lambda(\alpha,\beta)$ is the discrimination parameter of the noncentral χ^2 test at α and β levels. α and β are the first and second kind risk, or the type I and type II error (Koch and Link 1970), respectively [first kind risk = conclude concentration $C > 0$ when actually $C = 0$ (i.e., the true hypothesis is rejected); second kind of risk = conclude $C = 0$ when actually $C > 0$ (i.e., the false hypothesis has been accepted)]. For example, $\lambda(\alpha,\beta) = 13$, where $\alpha = \beta = 0.05$, indicates that t_{min} is given within 95% confidence level (Ancey et al. 1979).

Minimizing t_{min} requires the net count rate $I_C = I_P - I_B$ to be as large as possible. The following factors strongly influence the net count rate.

The probability of radiative transition related to the analyzed peak

This parameter is the product of the fluorescence yield (ω) times the relative transition probability (p) of the peak. Peaks with high energy (i.e., high ω) and high relative intensity (i.e., p close to unity) should be selected to enhance the detection limit.

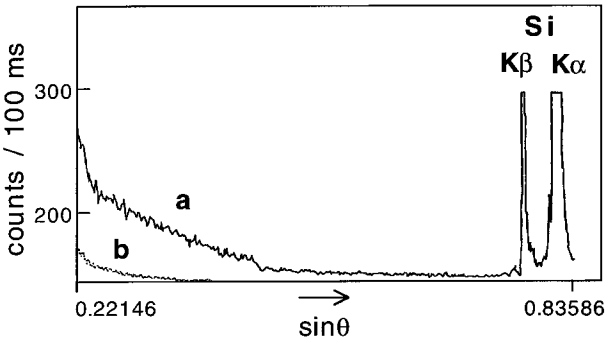

FIGURE 1. Full spectra acquired from a pure Si target at 35 kV and 500 nA. (**a**) Pulse height analyzer (PHA) off (integral mode). (**b**) PHA on (differential mode). In this example, the specular reflection BG is reduced by a factor four by selecting a PHA window 1.0 V wide and centered upon Cr*K*α ($\sin\theta = 0.26172$) to optimize the hypothetical search for Cr in pure Si. Most low energy photons that have undergone specular reflection from the monochromator surface are rejected by the PHA.

The intensity and the shape of the BG in the region of the analyzed peak

Three major components of the BG may be distinguished: (1) the so-called ''bremsstrahlung,'' which is the continuous X-ray spectrum generated by the deceleration of incident electrons within the sample; (2) the tails of neighboring peaks, which can exceed 1 keV on either side of a major peak; and (3) the specular reflection signal, which is due to the reflection of soft X-rays from the surface of monochromators. Specular reflection produces a signal that increases the BG at low Bragg angles (θ). This phenomenon is especially dramatic for the layered synthetic microstructured monochromators (LSM) used for light element analysis (Fialin et al. 1996). Figure 1 shows a spectrum emitted from pure Si as recorded with a PET monochromator over the full mechanical range of a wavelength dispersive spectrometer (WDS). The high-level BG at low Bragg angle is produced by the specular reflection of photons emitted from the low-energy part of the ''bremsstrahlung'' as well as those emitted in soft emission lines (e.g., Si $L_{II,III}$ with energy close to 100 eV). Proper setting of the pulse height analyzer (PHA) can reduce specular reflection background (b in Fig. 1).

The beam current and the accelerating potential E_0

The total number of X-ray photons generated within a bulk specimen depends upon the relationship between the ionization cross-section and E_0. The generated intensity is proportional to the overvoltage $(E_0 - E_c)^n$, where E_c is the excitation threshold potential for the analyzed line and $1 < n < 2$. The observed intensity is proportional to the product of the generation rate and the fraction of X-rays, $f(\chi)$, that escape the specimen surface at the fixed take-off angle Ψ. Hence, an incident energy E_p exists that produces the maximum observed intensity. E_p satisfies the relationship:

TABLE 1. Major element compositions of the reference glasses: EMP results compared to nominal values

	GSP-1		G2		BR		W-1		BCR-1		AGV-1	
	EMP	nominal	EMP	nominal	EMP	nominal	EMP	nominal	EMP	nominal	EMP	nominal
SiO_2 (wt%)	67.59	67.22	69.42	69.22	38.18	38.21	52.14	52.64	54.31	54.53	59.81	59.61
Al_2O_3	15.01	15.28	15.31	15.41	9.82	10.21	14.81	15.01	13.66	13.72	17.31	17.19
Fe_2O_3*	4.02	4.31	2.62	2.69	12.73	12.88	10.96	11.09	13.32	13.41	6.65	6.78
MnO	0.06	0.04	0.03	0.03	0.21	0.21	0.14	0.17	0.18	0.18	0.08	0.11
MgO	0.95	0.97	0.76	0.75	12.87	13.28	6.52	6.62	3.41	3.48	1.48	1.52
CaO	2.06	2.03	1.99	1.96	13.48	13.81	10.89	10.96	6.97	6.97	4.87	4.94
Na_2O	2.77	2.81	4.01	4.06	2.96	3.05	2.18	2.15	3.39	3.31	4.29	4.32
K_2O	5.47	5.51	4.54	4.46	1.37	1.41	0.66	0.64	1.71	1.71	3.01	2.92
TiO_2	0.66	0.66	0.51	0.48	2.74	2.61	1.05	1.07	2.19	2.26	1.06	1.06
P_2O_5	0.31	0.28	0.13	0.13	1.13	1.05	0.16	0.14	0.41	0.36	0.52	0.51
L.O.I.		0.72		0.71		3.66		0.73		1.59		1.81

Notes: Operating conditions: 15 kV (beam voltage), 10 nA (beam current), 10 μm (probe diameter). Standards used: diopside for Si, Ca, and Mg, orthoclase for Al and K, hematite for Fe, rhodonite for Mn and Ti, albite for Na, and apatite for P.
Fe_2O_3* = total iron as Fe_2O_3.

$$d[(E_0 - E_c)^n f(\chi)]/dE_0 = 0 \quad (6)$$

where $\chi = \mu \cdot \csc \Psi$ (μ is the mass absorption coefficient for the analyzed peak.

Based on a gaussian distribution of X-ray generation with depth, Kyser (1971) showed that E_p can be approximated as:

$$\chi = (2260/E_p)^{1.68}. \quad (7)$$

The instrumental resolution

The instrumental resolution controls the natural width of Bragg peaks and thus affects the peak-to-background ratio (PK/BG). Among factors affecting resolution, e.g., slits, alignment, and crystal perfection, we paid attention to the resolution of monochromators, which depends upon the number of reflecting planes encountered by the incident wave: the higher this number, the higher the resolution. Hence monochromators with low $2d$ spacings have improved resolution (LiF_{200} with $2d = 0.407$ nm is better than PET with $2d = 0.875$ nm), which provides the opportunity to achieve higher PK/BG ratios in cases where X-ray lines are closely spaced in energy.

EXPERIMENTAL PROCEDURE

Glass preparation

Starting materials were reference rock powders (Flanagan 1984) including granite (G-2), granodiorite (GSP-1), andesite (AGV-1), diabase (W-1) and several basalts (BCR-1, BR, and BE-N). Powders of each (about 2 g) were first dried at 110 °C for 1 h, producing aggregates that were then crushed in an agate mortar under alcohol. The samples were then placed in 10 cm^3 platinum crucibles, dehydrated at 700 °C for 2 h (loss of few milligrams of H_2O), and then heated to 1360 °C for a full fusion in a 25 min gradual heating process. This slow fusion method is required to prevent the loss of volatile components such as sulfate or carbonate, which in turn may promote a loss of alkaline elements (Na, K). Further details on the fusion process can be found in Schairer and Bowen (1955, 1956). Once melting was complete, crucibles were quenched in water to prevent crystallization (temperature reduced to 600 °C in 1–2 s). The glasses were crushed and fused again to improve the homogeneity. Finally, millimeter-sized grains were mounted in epoxy, polished with diamond paste (6, 3, and 1 μm), and carbon coated for EMP analysis.

Major/minor element analysis

Table 1 shows a favorable comparison between the measured concentrations of major elements and published values (Govindaraju 1989) obtained by different methods such as X-ray fluorescence and wet chemistry. Homogeneity tests also were successful. Major and minor element compositions were then used for matrix correction of trace elements.

EMP trace element methodology

To improve the detection limits of trace elements, a procedure was developed that includes fractional counting time, data statistical filtering, and BG modeling, as described below.

Measurements were performed on a Cameca SX 50 microprobe equipped with four WDS offering combinations of LiF_{200}, PET, TAP, and LSM monochromators. Eleven trace elements were analyzed using K, L, and M series peaks with energies ranging from 2 to 7 keV. By application of Equation 7, the optimal beam energy, E_p, was found to be 25–30 keV for peaks around 2 keV (Y*L*α, Zr*L*α, Sr*L*α, and Pb*M*α) and 80–110 keV for 5–7 keV peaks (Ni*K*α, rare earth L series). Because of technological limitations, beam energies above 40 keV are not feasible, and the value of 35 keV was therefore selected. At this energy and 500 nA, which is the upper limit for beam current regulation, the beam-excited area is about 80 μm^2, as estimated from the diameter (10 μm) of the cathodoluminescence-induced bright spot. Figure 2 shows the increase of the net count rate for the *K*α peaks of some low-concentration transition elements with increased beam voltage. With the above beam conditions (35 keV, 500 nA), 8 c/s are emitted by 10 ppm of these elements in a silicate matrix. The total counting time required to detect 10 ppm, $t_{tot} = t_{min} + t_B$, where the BG

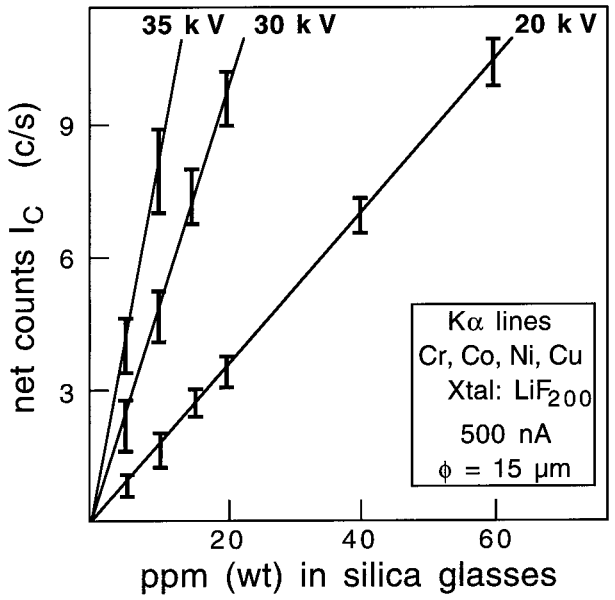

FIGURE 2. Plot of the net count rate, I_C, for *K*α peaks as a function of concentration for some transition metals in glasses. Bars ($\pm 2\sigma$) show the limits of average values for the selected elements. From Equation 7, higher values for I_C could be reached with accelerating voltages around 100 kV.

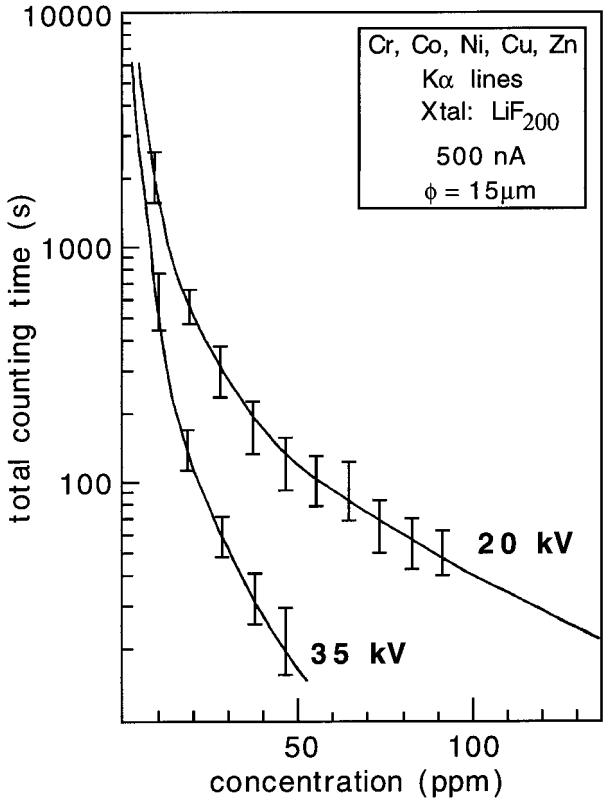

FIGURE 3. Total counting time, $t_{tot} = 2\ t_{min}$ (Eq. 5), required to attain specified detection limits for transition metals in silicate glasses. ϕ is the beam diameter.

counting time, t_B, is taken as identical with t_{min} (from Eq. 5), is on the order of 10 min (Fig. 3). For most analyzed peaks, except Ni*K*α, Pb*M*α, and Th*M*α, two crystal monochromators were available in which case the crystal with higher resolution was used. In addition, using LiF_{200} rather than PET for the rare earth L-peaks and PET rather than TAP for Y*L*α, Sr*L*α, and Zr*L*α, leads to higher Bragg angles for the analyzed peaks, which are thus located in spectral zones where the specular reflection BG is reduced.

The regular software (Cameca Quantiview, TR-type analyses[1]) was adapted to trace element determination by including two modifications to the analytical methods. (1) The selected counting time was divided into ten intervals, thus yielding ten PK and ten BG counts. Each set of counts was statistically processed through the χ^2 test and the filters of Dixon (1953) and Grubbs (1969), as recommended by Bodinier et al. (1987) and Merlet and Bodinier (1990). Finally, the averaged BG count values were subtracted from the PK values to obtain the net count rates. (2) A single analysis represents the average of data collected from a set of point analyses acquired in short counting times (10–20 s). This procedure reduces damage due to prolonged irradiation of beam-sensitive materials such as apatites and alkali-rich glasses. The sample is automatically moved between measurements to sites previously stored by the operator. The probed area thus represents the sum of all point analysis surfaces. This severely limits the spatial resolution of the method and also requires the sample to be homogeneous at the trace level. This mode is referred to as ''multi-site'' mode. Here again, each PK and BG subset was processed statistically prior to being accumulated to yield the PK and BG count rate.

The precision of measured concentrations ($\pm 2\sigma$) was calculated from the following formula:

$$\Delta C/C = [(\Delta k_S)^2 + (\Delta k_B)^2]^{1/2}/k. \quad (8)$$

Δk_S is the statistical error on the k-ratios [$k = (I_P - I_B)/(I_{Ps} - I_{Bs})$] related to low concentrations, as deduced from the general formula of Ancey et al. (1979):

$$\Delta k_S = (3.84 \cdot I_P \cdot t)^{1/2}/(I_{Ps} \cdot t) \quad (9)$$

where I_{Ps} and I_{Bs} are the count rates for the standard PK and BG, respectively. Δk_S is proportional to $\sqrt{t}$.

Δk_B is a term of systematic uncertainty designed to evaluate the loss in accuracy due to the lack of precise knowledge of the BG profile. This uncertainty is generally eliminated by trying to use standards with ''zero'' concentration and measuring BG at the PK position. This is only feasible in special materials. In practice, Δk_B is evaluated from the comparison of both net count rates $I_P - I_B$ and $I_P - I_{Blin}$. Δk_B is taken as:

[1] Code modifications to the analytical software are in progress at Cameca for the commercial package.

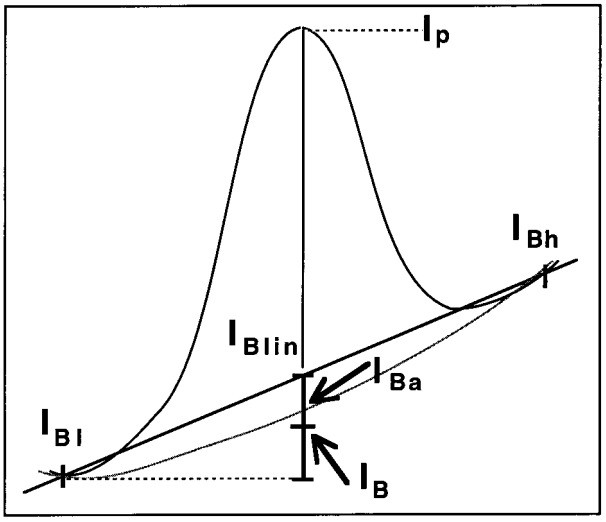

FIGURE 4. Sketch of a low-intensity PK on a smooth and concave shaped BG. $I_B = (I_{Blin} + I_{Bl})/2$ is taken as the measured BG. I_{Blin} is deduced from linear interpolation between two values, I_{Bl} anb I_{Bh}, collected within a range 250–400 steps (1 step = $2 \cdot 10^{-5}$ sinθ) on either sides of the PK. I_{Ba} is the actual BG, not directly accessible. The bold bar shows the limits where I_{Ba} is expected. The subsequent uncertainty on the k-ratio is expressed by Equation 10. I_p is the peak intensity.

$$\Delta k_B = 0.95\ (k_{lin} - k) \qquad (10)$$

where $k_{lin} = (I_p - I_{Blin})/(I_{Ps} - I_{Bs})$. The latter parameters are schematically defined in Figure 4.

RESULTS

The multi-site mode was used. Tests for beam damage are shown in Figure 5, using four elements with sufficient concentrations to be detected with counting times of 20 s (Ni = 75 ppm and Zr = 99 ppm in glass W-1; Nd = 65 ppm in BR; and Th = 106 ppm in GSP-1). Despite obvious changes in the glass aspect, in particular those described by Lineweaver (1963) such as electron browning and surface displacement in the direction of bombarding electrons, count rates remained stable over long time periods. Eventual discrepancies, due to the migration of the trace elements, lie within the data scattering due to counting statistics. Presumably, beam damage involving mobilization of the more volatile components (e.g., the alkalies or oxygen) does not affect the trace element measurements, hence the trace elements are comparatively immobile.

Trace element results are compared to nominal data in Figure 6 and mean results are summarized in the abstract. Excellent agreement is seen at concentrations >80 ppm for Ni and Cr, >100 ppm for La and Nd, >130 ppm for Zr, Ce, and Th, and >200 ppm for Sr. In all of these cases, the EMP data are within ±10% of reference values. At lower concentrations (13 to 55 ppm depending on the element), the precision (±2σ) remains below 50%. The detection limits are also reported on Figure 6. It should be noted that improvement of the detection limit for Sr at concentrations <150 ppm requires precise BG modeling due to the proximity of the Si*K*α peak to Sr*L*α.

Comparison of these results with the PIXE and SXRF data reported by Mosbah et al. (1995) for synthetic and natural volcanic glasses shows similar detection limits for transition metal analysis. SXRF gives improved values for some elements (Koch and Link 1970; e.g., 1.6 ppm for Ni) but the analyzed depth is above 80 μm (30–35 μm for PIXE) compared to a few micrometers for the EMP.

CONCLUDING REMARKS AND PERSPECTIVES

This paper has shown the feasibility of trace element analysis by EMP and should encourage the use of the

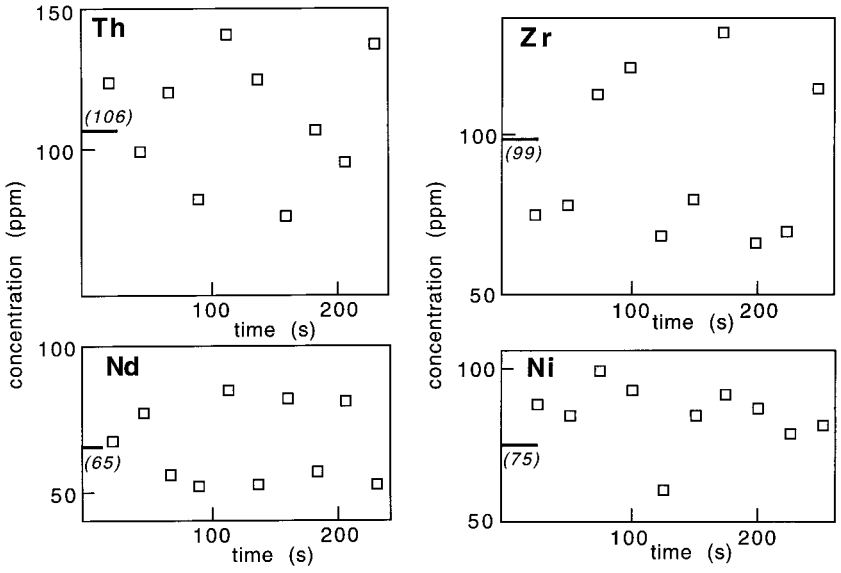

FIGURE 5. Beam damage tests. Plots were made using data from ten consecutive analyses on a single site. Six runs collected from distinct sites were averaged to improve precision. Error bars were omitted for clarity. The bold bar on the Y axis refers to the nominal value given in parenthesis.

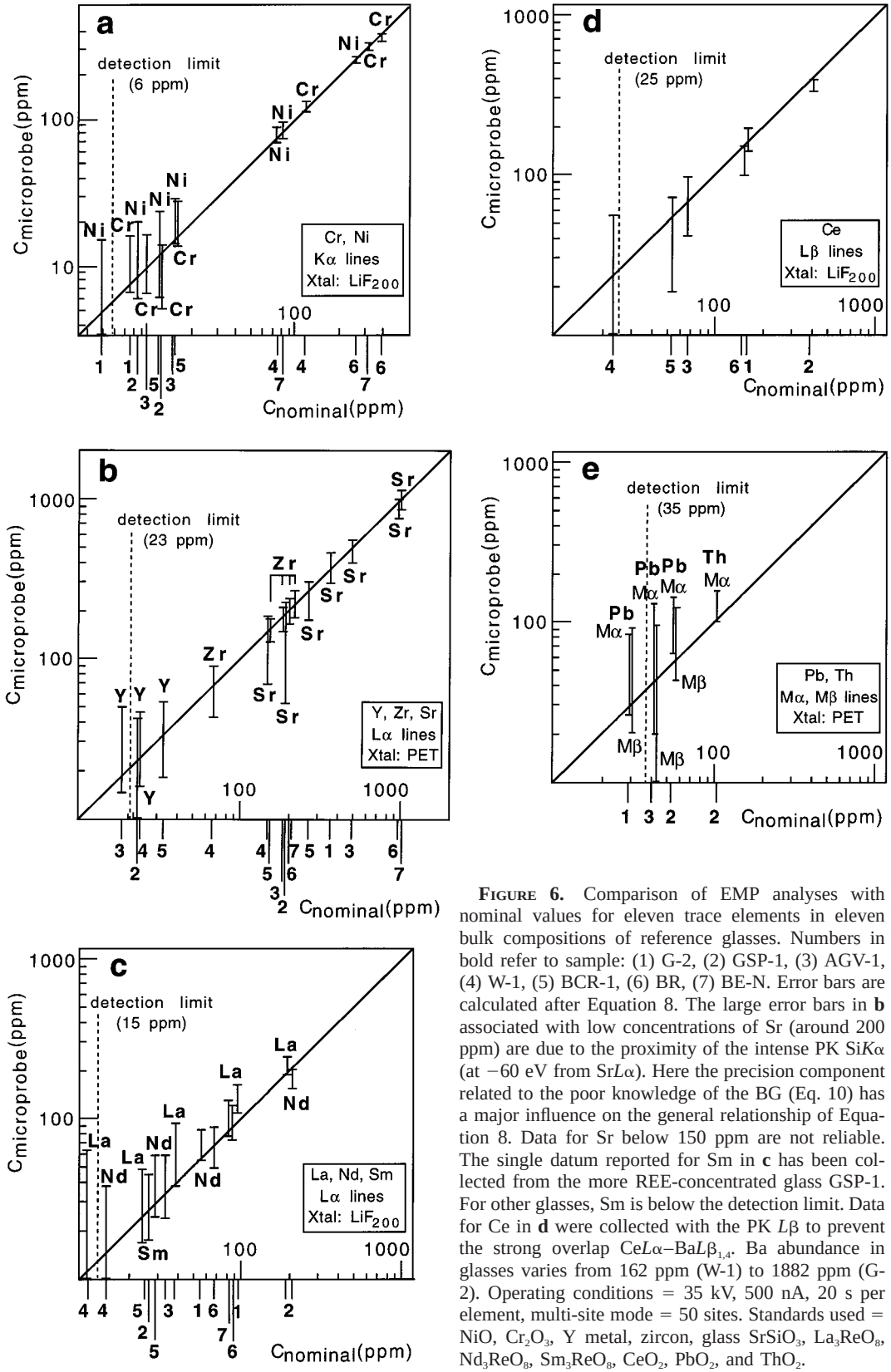

FIGURE 6. Comparison of EMP analyses with nominal values for eleven trace elements in eleven bulk compositions of reference glasses. Numbers in bold refer to sample: (1) G-2, (2) GSP-1, (3) AGV-1, (4) W-1, (5) BCR-1, (6) BR, (7) BE-N. Error bars are calculated after Equation 8. The large error bars in **b** associated with low concentrations of Sr (around 200 ppm) are due to the proximity of the intense PK Si$K\alpha$ (at −60 eV from Sr$L\alpha$). Here the precision component related to the poor knowledge of the BG (Eq. 10) has a major influence on the general relationship of Equation 8. Data for Sr below 150 ppm are not reliable. The single datum reported for Sm in **c** has been collected from the more REE-concentrated glass GSP-1. For other glasses, Sm is below the detection limit. Data for Ce in **d** were collected with the PK $L\beta$ to prevent the strong overlap Ce$L\alpha$–Ba$L\beta_{1,4}$. Ba abundance in glasses varies from 162 ppm (W-1) to 1882 ppm (G-2). Operating conditions = 35 kV, 500 nA, 20 s per element, multi-site mode = 50 sites. Standards used = NiO, Cr_2O_3, Y metal, zircon, glass $SrSiO_3$, La_3ReO_8, Nd_3ReO_8, Sm_3ReO_8, CeO_2, PbO_2, and ThO_2.

EMP to approach concentrations as low as a few parts per million. Owing to the easy use and high degree of automation of modern EMP's, preliminary studies on trace element abundance by this method are technically attractive and useful. Lower detection limits and better accuracy and precision on measurements could then be achieved on EMP-selected samples by the more elaborate techniques listed in the introduction.

We currently apply the methods described here to mantle minerals including REE-bearing phases, apatite, and titanite, and to clinopyroxenes (the major host of Sr and REE in lherzolites). These phases reveal the environment of crystallization (silicate/carbonate melt/fluid) and are especially important to the understanding of geochemical processes. REE have been analyzed in apatites using the multi-site mode with adapted beam conditions (30 kV, 150 nA). Concentrations of heavy-REE (HREE), (e.g., Er and Gd) on the order of 150–300 ppm were determined with rather good precision (2σ = 10–20%), with cumulative counting times of 20–30 min.

Comparative and complementary studies using alternative methods for chemical analysis remain essential. We have focused on analysis of synthetic glasses in the present work. Some comparative studies of minerals may be found in the literature: a EMP/PIXE study on sulfides (Rémond et al. 1987); an original study of argon sorption in quartz (Roselieb et al. 1997) with combined data from gas chromatography, Knudsen cell mass spectroscopy and the EMP (detection limit of 30 ppm with the Ar$K\alpha$ peak at 15 kV). The EMP has been compared successfully to the technique of laser-ablation, inductively coupled plasma-mass spectroscopy (LA-ICP-MS) for analyzing zircons and apatites (Sère 1996). We have recently initiated a EMP/SIMS/neutron activation comparative study of incompatible (La, Ce, Sr, and Nd) and compatible (Zr, Y) elements in LREE-enriched pyroxenes from alkali clinopyroxenite xenoliths (Wagner and Fialin 1998). Preliminary data show concentrations as low as 20–40 ppm (2σ = 50%), results which are in good agreement with SIMS data; traverse profiles (one point every 6–8 μm) in zoned crystals reveal a sharp boundary between the cores and outer mantling zones. A major advantage of the EMP over other microbeam techniques is the improved spatial resolution (a SIMS impact crater is not less than 40 μm). Finally, cathodoluminescence (CL) spectroscopy should be cited as a complementary technique to the EMP for a rapid qualitative identification of trace elements acting as luminescence-activating ions (transition metals, REE, actinides) in phosphates, carbonates, and particularly silicates (Rémond et al. 1992). Recently, Baumer et al. (1997) have shown that CL may be sensitive down to 1 ppm or less for HREE.

Acknowledgments

H.R. is indebted to Pascal Richet (IPGP-University of Paris VII) for his help with the powder fusion procedures. We acknowledge a careful review by R.J. Tracy (Virginia Tech) and thank the reviewers George B. Morgan VI (University of Oklahoma) and Ian Steele (University of Chicago) for their constructive criticism that improved the manuscript. Financial support provided by the Centre de Microanalyse Camparis.

References cited

Ancey, M., Bastenaire, F., and Tixier, R. (1979) Application of statistical methods in microanalysis. In F. Maurice, L. Meny, and R. Tixier, Eds., Microanalysis and scanning electron microscopy, p. 319–343. Les Editions de Physique, Orsay, France.

Baumer, A., Blanc, P., Cesbron, F., and Ohnenstetter, D. (1997) Cathodoluminescence of synthetic (doped with rare-earth elements) and natural anhydrites. Chemical Geology, 138, 73–80.

Bodinier, J-L., Dupuy, C., Dostal, J., and Merlet, C. (1987) Distribution of trace transition elements in olivine and pyroxenes from ultramafic xenoliths: Application of microprobe analysis. American Mineralogist, 72, 902–913.

Dixon, W.J. (1953) Processing data for outliers. Biometrics, 9, 74–89.

Fialin, M., André, J-M., Chauvineau, J-P., Rousseaux, F., Ravet, M-F., Decanini, D., Cambril E., and Rémy, H. (1996) Extending the possibilities of soft X-ray spectrometry through the etching of layered synthetic microstructure monochromators. X-ray Spectrometry, 25, 60–65.

Flanagan, F.J. (1984) Reference samples in Geology and in Geochemistry. U.S. Geological Survey Bulletin 1582, 70 p. Geostandards Newsletter, 10, 191–264.

Goldstein, J.I., Williams, D.B., and Cliff, G. (1986) Quantitative X-ray analysis. In D.C. Joy, A.D. Romig, and J.I. Goldstein, Eds., Principles of analytical electron microscopy, p. 155–217. Plenum Press, New York.

Govindaraju, K. (1989) 1989 compilation of working values and sample description for 272 geostandards. Geostandards Newsletter, XIII, Special issue, 1–113.

Grubbs, F.E. (1969) Procedure for detecting outlying observations in samples. Technometrics, 11, 1–21.

Johnson, K.E., Davis, A.M., and Bryndzia, L.T. (1996) Contrasting styles of hydrous metasomatism in the upper mantle: an ion microprobe investigation. Geochemica et Cosmochimica Acta, 60, 1367–1385.

Koch, G.S., Jr. and Link, R.F. (1970) Statistical Analysis of Geological Data, p. 106–107. Wiley, New York.

Kyser, D.F. (1971) Experimental determination of mass absorption coefficients for soft X-rays. In G. Shinoda, K. Kohra, and T. Ichinokawa, Eds., Proceedings of the Sixth International Conference on X-ray Optics and Microanalysis, p. 147–156. University of Tokyo Press, Japan.

Lineweaver, J.L. (1963) Oxygen outgassing caused by electron bombardment of glasses. Journal of Applied Physics, 34, 1786–1791.

Lloyd, F.E., Edgar, A.D., and Ragnarsdottir, K.V. (1996) LREE distribution in perovskite, apatite and titanite from South West Ugandan xenoliths and kamafugite lavas. Contributions to Mineralogy and Petrology, 57, 205–228.

Merlet, C. and Bodinier, J-L. (1990) Electron microprobe determination of minor and trace transition elements in silicate minerals: A method and its application to mineral zoning in the peridotite nodule PHN 1611. Chemical Geology, 83, 55–69.

Mosbah, M., Clocchiatti, R., Michaud, V., Piccot, D., Chevallier, P., Legrand, F., Als Nilsen, G., and Grübel, G. (1995) Micro PIXE and micro SXRF: comparison of the two methods and application to glass inclusions from Vulcano (Eolian Islands-Italy). Nuclear Instruments and Methods in Physics Research B, 104, 481–488.

Reed, S.J.B. (1995) Wavelength dispersive spectrometry-A review. In D.B. Williams, J.I. Goldstein, and D.E. Newbury, Eds., X-Ray spectrometry in electron beam instruments, 390 p. Plenum Press, New York.

Rémond, G., Cesbron, F., Traxel, K., Campbell, J.L., and Cabri, L.J. (1987) Electron microprobe analysis and proton induced X-ray spectrometry applied to trace element analysis in sulfides: problems and prospects. Scanning Microscopy, 1, 1017–1037.

Rémond, G., Cesbron, F., Chapoulie, R., Ohnenstetter, D., Roques-Carmes, C., and Schvoerer, M. (1992) Cathodoluminescence applied to the microcharacterisation of mineral materials: a present status in experimentation and interpretation. Scanning microscopy, 6, 23–68.

Roselieb, K., Blanc, P., Büttner, H., Jambon, A., Rammensee, W., Rosenhauer, M., Vielzeuf, D., and Walter, H. (1997) Experimental study of

argon sorption in quartz: Evidence for argon incompatibility. Geochemica et Cosmochimica Acta, 61, 533–542.

Schairer, J.F. and Bowen, N.L. (1955) The system K_2O-Al_2O_3-SiO_2. American Journal of Science, 253, 681–746.

———(1956) The system Na_2O-Al_2O_3-SiO_2. American Journal of Science, 254, 129–195.

Sère, V. (1996) Géochimie des minéraux néoformés à Oklo (Gabon), histoire géologique du bassin d'Oklo : une contribution pour les études de stockage géologiques de déchets radioactifs, 280 p. Thèse de l'Université Paris VII, Université Paris VII, Paris, France.

Vannucci, R., Ottolini, L., Bottazzi, P., Downes, H., and Dupuy, C. (1994) INAA, IDMS and SIMS comparative investigations of clinopyroxenes from mantle xenoliths with different textures. Chemical Geology, 118, 85–108.

Wagner, C. and Fialin M. (1998) LREE- and Sr-enriched clinopyroxenes in pyroxenite xenoliths from North Morocco: an EPMA investigation. Proceedings EMPG VII, Orléans, France.

Manuscript received January 20, 1998
Manuscript accepted August 25, 1998
Paper handled by Robert J. Tracy